Ionic Liquid–solute Interactions Studied by 2D-NOE NMRSpectroscopy.

ARTICLE *in* THE JOURNAL OF PHYSICAL CHEMISTRY B · NOVEMBER 2014

Impact Factor: 3.3 · DOI: 10.1021/jp509861g · Source: PubMed

THE JOURNAL OF PHYSICAL CHEMISTRY B

Article

pubs.acs.org/JPCB

Ionic Liquid–Solute Interactions Studied by 2D NOE NMR Spectroscopy

Sufia Khatun and Edward W. Castner, Jr.*

Department of Chemistry and Chemical Biology, Rutgers, The State University of New Jersey, Piscataway, New Jersey 08854, United States

Supporting Information

ABSTRACT: Intermolecular interactions between a $Ru^{2+}(bpy)_3$ solute and the anions and cations of four different ionic liquids (ILs) are investigated by 2D NMR nuclear Overhauser effect (NOE) techniques, including $\{^1H-^{19}F\}$ HOESY and $\{^1H-^1H\}$ ROESY. Four ILs are studied, each having the same bis(trifluoromethylsulfonyl)amide anion in common. Two of the ILs have aliphatic 1-alkyl-1-methylpyrrolidinium cations, while the other two ILs have aromatic 1-alkyl-3-methylimidazolium cations. ILs with both shorter (butyl) and longer (octyl or decyl) cationic alkyl substituents are studied. NOE NMR results suggest that the local environment of IL anions and cations near the $Ru^{2+}(bpy)_3$ solute is rather different from the bulk IL structure. The solute–anion and solute–cation interactions are significantly different both for ILs with short vs long alkyl tails and for ILs with aliphatic vs aromatic cation polar head groups. In particular, the solute–anion interactions are observed to be about 3 times stronger for the cations with shorter alkyl tails relative to the ILs with longer alkyl tails. The $Ru^{2+}(bpy)_3$ solute interacts with both the polar head and the nonpolar tail groups of the 1-butyl-1-methylpyrrolidinium cation but only with the nonpolar tail groups of the 1-decyl-1-methylpyrrolidinium cation.

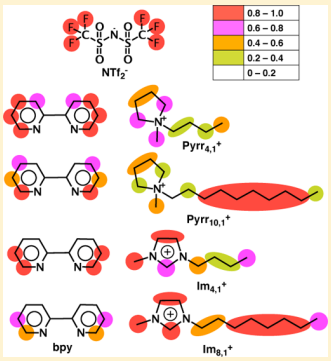

INTRODUCTION

The diversity of ionic liquid (IL) anions and cations offers significant advantages for their use as designer solvents. Some of the unique chemical, biochemical, and materials applications for ILs include organic, organometallic, and enzymatic catalysis;[1−3] electrochemical applications, including solar photoelectrochemical cells and improved batteries;[4,5] pretreatment of lignocellulosic biomass for liquid fuels,[6−8] gas and liquid separations, including sequestration of carbon dioxide,[9−11] and synthesis of nanomaterials, polymers, catalysts, and pharmaceuticals.[12−14] ILs may ultimately prove useful for a wide array of energy applications.[15]

The amphiphilic properties of IL anions or cations means that they are significantly more ordered than neutral solvents. The local structure and intermediate range order have been widely studied for neat ILs.[16−34] Recent work using molecular dynamics simulations, neutron and X-ray diffraction, NMR spectroscopy, and theoretical chemistry has provided significant insight into the structure and dynamics of ionic liquids.[16−21,31−42] Several groups of researchers have worked to understand mixtures of ILs with common solvents such as water, benzene, and butane.[43−50] Other researchers have investigated how the use of ILs as solvents affects the mechanisms and rates of chemical reactions.[51−62] Taken together, the ever-expanding body of work on ILs shows that the physical properties of ILs are very different from neutral solvents, as are their effects on chemical and biochemical processes in solution.

Many of the energy-related applications of ILs make use of the fact that they are intrinsic electrolytes that can facilitate electron- and proton-transfer reactions.[15,51] A fundamental question in ionic liquids research is then, how is the bulk liquid structure of an IL changed in the immediate environment of a solute? The structure of neat ILs shows a charge ordering for adjacent nearest-neighbor ions that alternates between anions and cations. However, molecular simulations provide a growing body of evidence that the solvation structure of anions and cations surrounding a solute is significantly different. One approach to studying specific solvation effects in ionic liquids has been to apply extended X-ray absorption fine structure (EXAFS) spectra of metal complexes dissolved in ionic liquid solutions.[63] Recent simulations by Terranova and Corcelli provided the partial radial pair distribution functions between the centers of masses of the coumarin 153 (C153) solvatochromic probe molecule and the IL anions and cations. Their results provide a picture of the first solvation shell surrounding the C153 solute that is enriched in 1-ethyl-3-methylimidazolium ($Im_{2,1}^+$) cations, while the second shell shows an increased probability density for finding the tetrafluoroborate (BF_4^-) anions.[64] This is not the first report for such specific solvation, as evidence for a similar preferential distribution of $Im_{4,1}^+$ cations comprising the first solvation shell about a betaine-30 solvatochromic probe molecule with the PF_6^- anions dominating the second shell was discussed by Znamenskiy and Kobrak.[65] More generally, it seems clear that

Special Issue: Branka M. Ladanyi Festschrift

Received: September 29, 2014
Revised: November 16, 2014

   dx.doi.org/10.1021/jp509861g | J. Phys. Chem. B XXXX, XXX, XXX–XXX

the distributions of anions and cations in the first solvation shell for a neutral solute in an IL solution are likely to be very different than those for a charged solute. These studies from Znamenskiy and Kobrak and Terranova and Corcelli point to the need for experimental evidence about the nature of the ionic liquid structure in a solution, since this structure is likely to be different than that for the neat bulk fluid.[64,65]

In this work, we probe the nature of the local solvation environment surrounding the prototypical photosensitizer $Ru^{2+}(bpy)_3Cl_2^-$. Using 2D nuclear Overhauser effect (NOE) NMR experiments, we examine the specific interactions between ionic liquid (IL) anions and cations and the $Ru^{2+}(bpy)_3$ solute. From these experiments, we learn that the chemical nature of the anions and cations leads to very different arrangements of ions surrounding the solute molecules. The structures of the $Ru^{2+}(bpy)_3$ solute, the bpy ligand, and the IL anion and cations we have studied are shown in Figure 1.

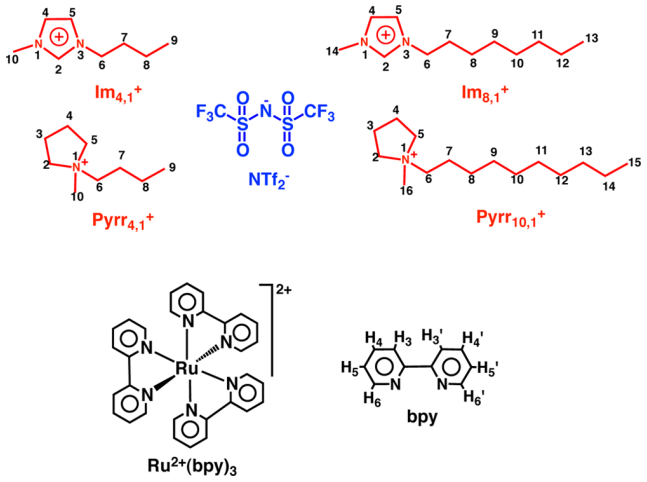

Figure 1. Chemical structures of IL cations, the NTf_2^- anion, and the $Ru^{2+}(bpy)_3$ solute.

2D NMR experiments exploiting the nuclear Overhauser effect (NOE) are widely used to study intermolecular interactions in liquids and solids.[66−78] Specifically, 2D NMR techniques such as $\{^1H-^{19}F\}$ HOESY and $\{^1H-^1H\}$ ROESY are frequently used to investigate interactions between nuclei that are in close proximity. The HOESY pulse sequence provides a measure of the strength of interactions between heteronuclear spins, thus providing information on intermolecular anion−cation and solute−anion interactions. The ROESY pulse sequence is a homonuclear Overhauser technique that provides information on intermolecular cation−cation and solute−cation interactions. The groups of Mele and Giernoth have shown that such NOE methods can successfully be applied to the study of intermolecular interactions in ionic liquids.[71,72,76,78]

The four different ILs used in these experiments include two aromatic imidazolium and two nonaromatic pyrrolidinium cations, with each cation paired with the bis(trifluoromethylsulfonyl)amide (NTf_2^-) anion. Longer alkyl tails on either cations or anions lead to the formation of nanometer scale hydrophobic domains that alternate with polar domains.[79] These ILs are chosen because of their good temperature stability and because they have broad windows of electrochemical stability.[80] The $Ru^{2+}(bpy)_3$ photosensitizer has a long and distinguished history for use as a photocatalyst and sensitizer for solar photoelectrochemical cells. Seminal articles on this photosensitizer are available,[81,82] and include a discussion of solvent effects.[83] Recently, $Ru^{2+}(bpy)_3$ was used in an ionic liquid polymer gel electrolyte as the electrochemiluminescent species for flexible displays.[84]

EXPERIMENTAL METHODS

Sample Preparation. All ionic liquids were ultrahigh purity grade purchased from IoLiTec. Before vacuum purification, we determined that the purity levels were 99.7%; this value increased on removal of trace quantities of volatile water and dichloromethane. The $Ru^{2+}(bpy)_3Cl_2^-$ solutions were prepared at 40 mM concentration, the solubility limit for this species in some of the ILs. The $Ru^{2+}(bpy)_3Cl_2^-$ was purchased from Sigma-Aldrich and used as received. The IL solutions were dried under a vacuum at a pressure of 10^{-2} Torr for 48 h and transferred to 2.5 mm capillary NMR tubes inside an argon glovebox. The NMR capillary tubes were first capped with beeswax and then immediately flame-sealed after removal from the glovebox. The sealed 2.5 mm capillary tubes containing the samples were placed inside a 5 mm outer diameter NMR tube containing 99.9% D_2O solvent to provide a deuterium lock signal for the 2D HOESY and ROESY experiments. Prior to drying the ILs, the 1D ^1H NMR spectra show a water peak at 2.67 ppm for the IL solutions with pyrrolidinium cations and a water peak at 2.73 ppm for solutions with imidazolium cations. The water peak disappeared from the ^1H spectra after drying. Our ^1H experiments on trace water in $Im_{4,1}^+/NTf_2^-$ show that the NMR limit of detection is below 50 ppm of H_2O by mass, so we estimate the water content of our dried samples to be significantly below 50 ppm in the flame-sealed NMR tubes.

NMR Measurements. All HOESY and ROESY experiments were performed at ambient temperature. 2D HOESY and ROESY experiments were done using Varian DirectDrive spectrometers with 300 and 400 MHz ^1H frequencies. The $\{^1H-^{19}F\}$ HOESY spectra were obtained using a pulsed field gradient inverse HOESY sequence with 128 increments of t_1 and 120 ms mixing times using 16 scans.[77] The $\{^1H-^1H\}$ ROESY spectra were measured using a pulsed field gradient ROESY sequence with 128 increments of t_1, 64 scans, and 200 ms mixing time. The ROESY pulse sequence included a two-pulse spin lock, repeated 766 times. 1D NOE intensities were measured for an array of delay times for each IL−solute sample to optimize the mixing time for the 2D $\{^1H-^{19}F\}$ HOESY experiments. Following analysis of these NOE intensities, a 120 ms mixing time was selected for the HOESY experiments to optimize the balance between minimizing the effects of spin diffusion while maximizing the signal-to-noise ratio and intensities of the 2D NOE spectra. For the ROESY experiments, the $^1H-^1H$ NOE intensity was optimized as a function of mixing time to the maximal intensity at 200 ms. Further details regarding optimization of the NMR pulse parameters and subsequent analysis of the 2D NOE spectra are provided in the Supporting Information.

Analysis of 2D NOE Spectra. To interpret the HOESY and ROESY spectra, the cross-peak intensities were obtained from volume integrations using Mnova software (MestreLabs, version 8.1).[85] The integrated HOESY intensities were corrected by a factor of $n_H n_F/(n_H + n_F)$, and the analogous ROESY intensities were corrected by $n_{Ha} n_{Hb}/(n_{Ha} + n_{Hb})$, where n_H is the number of equivalent ^1H nuclei contributing to the observed NOE signal and n_F is the corresponding number of equivalent ^{19}F nuclei.[71,86] Because each sample has a

dx.doi.org/10.1021/jp509861g | J. Phys. Chem. B XXXX, XXX, XXX−XXX

Table 1. Integrated Peak Volume of All Observed $\{^1H-^{19}F\}$ HOESY Cross-Peaks of $Ru^{2+}(bpy)_3$ in $Pyrr_{4,1}^+/NTf_2^-$ and $Pyrr_{10,1}^+/NTf_2^-$ at 120 ms Mixing Time[a]

			$Ru^{2+}(bpy)_3$ and $Pyrr_{4,1}^+/NTf_2^-$ Solution				
	n_H	n_Hn_F/N	I_{raw}	$I_{raw}N/(n_Hn_F)$	C_{corr}	I_{corr}	$I_{corr,N}$
				$Pyrr_{4,1}^+$			
H(2,5)	4	2.4	6.71	2.80	1.00	2.80	0.68
H(3,4)	4	2.4	6.11	2.55	1.00	2.55	0.52
H(6)	2	1.5	1.71	1.14	1.00	1.14	0.28
H(7)	2	1.5	1.78	1.19	1.00	1.19	0.29
H(8)	2	1.5	1.84	1.23	1.00	1.23	0.30
H(9)	3	2.0	4.84	2.42	1.00	2.42	0.51
H(10)	3	2.0	7.49	3.75	1.00	3.75	0.69
				bpy			
$H_3/H_{3'}$	6	3.0	0.12	0.040	82.50	3.30	0.80
$H_4/H_{4'}$	6	3.0	0.15	0.050	82.50	4.13	1.00
$H_5/H_{5'}$	6	3.0	0.15	0.050	82.50	4.13	1.00
$H_6/H_{6'}$	6	3.0	0.15	0.050	82.50	4.13	1.00
			$Ru^{2+}(bpy)_3$ and $Pyrr_{10,1}^+/NTf_2^-$ Solution				
	n_H	n_Hn_F/N	I_{raw}	$I_{raw}N/(n_Hn_F)$	C_{corr}	I_{corr}	$I_{corr,N}$
				$Pyrr_{10,1}^+$			
H(2,5)	4	2.4	1.67	0.70	1.00	0.70	0.40
H(3,4)	4	2.4	2.32	0.97	1.00	0.97	0.55
H(6)	2	1.5	0.48	0.32	1.00	0.32	0.18
H(7)	2	1.5	0.60	0.40	1.00	0.40	0.23
H(8–14)	14	4.2	7.37	1.75	1.00	1.75	1.00
H(15)	3	2.0	1.38	0.69	1.00	0.69	0.39
H(16)	3	2.0	1.57	0.79	1.00	0.79	0.45
				bpy			
$H_4/H_{4'}$	6	3.0	0.06	0.020	62.50	1.25	0.71
$H_5/H_{5'}$	6	3.0	0.05	0.017	62.50	1.04	0.60
$H_6/H_{6'}$	6	3.0	0.07	0.023	62.50	1.46	0.83

[a] n_H and n_F are the number of protons and fluorines in solution; $n_F = 6$ and $N = n_H + n_F$. I_{raw} is the integrated volume. The concentration correction factor (C_{corr}) is unity for the neat ILs and is defined as the ratio of solute to IL molarities ([IL]/[solute]) for bpy peaks. The concentration correction intensity is $I_{corr} = C_{corr}I_{raw}N/(n_Hn_F)$, and the normalized corrected intensity is $I_{corr,N} = I_{corr}/\max(I_{corr})$.

$Ru^{2+}(bpy)_3$ concentration of 40 mM, the corrected integrated intensities of HOESY and ROESY cross-peaks were multiplied by the concentration correction factors for each IL–$Ru^{2+}(bpy)_3$ solution, which range between 62.5 and 85.0, based on the densities of the respective ILs. The concentration corrected intensities were scaled for each solution and are shown in Tables 1 and 2 in the body of the manuscript.

RESULTS AND DISCUSSION

Though ionic liquids can behave as Newtonian fluids at higher temperatures, the combination of strong electrostatic interactions between ions together with local aggregation of nonpolar parts of amphiphilic ions leads to strongly ordered liquid structures. The structure of neat ILs has been reported on the basis of X-ray and neutron diffraction experiments[17,19,20,25,87] as well as from molecular dynamics simulations[22−24,31,34,88−91] and Raman and optical Kerr spectroscopy.[52,92−97]

NMR experiments provide an alternate perspective on the structure and interactions between ions in ILs. The nuclear Overhauser effect permits study of the interactions between species in solution. Heteronuclear 2D NOE spectroscopy (HOESY) has been used to probe interactions between ILs with cations containing only ^1H but not ^{19}F nuclei while using anions devoid of ^1H nuclei but having ^{19}F nuclei. 2D NMR NOE cross-peaks normally result from dipolar cross-relaxation of neighboring spins through space. Thus, NOE signal intensities are a function of the distances between interacting nuclei.[86]

For liquid samples with rapid solvent relaxation, such as aqueous protein solutions, the spectral density functions that determine the NOE signal intensities typically show a sharp dependence on the distance between interacting spins that varies as r^{-6}.[67,98] Gabl, Weingaertner, and Steinhauser have shown that for neat ILs, the distance dependence of the NOE signal between interacting spins may vary between r^{-6} and r^{-1}.[99,100]

Castiglione et al. studied ILs having the $Pyrr_{4,1}^+$ cation paired with NTf_2^- and bis(pentafluoroethylsulfonyl)imide, which illustrated that specific proton groups on the $Pyrr_{4,1}^+$ cation interacted strongly with the ^{19}F nuclei on the anions, while other protons did not.[71] A further study by Castiglione et al. showed that for the same cation paired with three different fluorinated anions, the interactions were significantly different.[72] They interpreted these results to indicate the existence of local phase segregation between the alkyl vs the perfluoroalkyl groups. Lingscheid et al. investigated the cation–anion interactions between $Im_{2,1}^+/BF_4^-$, $Im_{4,1}^+/BF_4^-$, and $Im_{4,1}^+/PF_6^-$ by measuring the HOESY spectra both in the neat IL and in solutions of CD_2Cl_2 and d_6-DMSO. They observed that, for the two ILs with the $Im_{4,1}^+$ cation, the more acidic proton at the 2-position of the imidazolium ring showed the strongest interactions with the ^{19}F atoms of the anion. NMR studies of the neutral deuterated solvents showed the expected ion-pairing

dx.doi.org/10.1021/jp509861g | J. Phys. Chem. B XXXX, XXX, XXX–XXX

Table 2. Integrated Peak Volume of All Observed $\{^1H-^{19}F\}$ HOESY Cross-Peaks of $Ru^{2+}(bpy)_3$ in $Im_{4,1}^+/NTf_2^-$ and $Im_{8,1}^+/NTf_2^-$ Solutions at 120 ms Mixing Time[a]

			$Ru^{2+}(bpy)_3$ and $Im_{4,1}^+/NTf_2^-$ Solutions				
	n_H	n_Hn_F/N	I_{raw}	$I_{raw}N/(n_Hn_F)$	C_{corr}	I_{corr}	$I_{corr,N}$
				$Im_{4,1}^+$			
H(2)	1	0.9	2.94	3.27	1.00	3.27	0.72
H(4,5)	2	1.5	5.55	3.70	1.00	3.70	0.81
H(6)	2	1.5	3.52	2.35	1.00	2.35	0.51
H(7)	2	1.5	2.52	1.68	1.00	1.68	0.37
H(8)	2	1.5	2.38	1.59	1.00	1.59	0.35
H(9)	3	2.0	5.54	2.77	1.00	2.77	0.61
H(10)	3	2.0	9.12	4.56	1.00	4.56	1.00
				bpy			
$H_5/H_{5'}$	6	3.0	0.15	0.05	85.00	4.25	0.93
$H_6/H_{6'}$	6	3.0	0.15	0.05	85.00	4.25	0.93
			$Ru^{2+}(bpy)_3$ and $Im_{8,1}^+/NTf_2^-$ Solutions				
	n_H	n_Hn_F/N	I_{raw}	$I_{raw}N/(n_Hn_F)$	C_{corr}	I_{corr}	$I_{corr,N}$
				$Im_{8,1}^+$			
H(2)	1	0.9	1.49	1.66	1.00	1.66	0.84
H(4,5)	2	1.5	2.74	1.83	1.00	1.83	0.92
H(6)	2	1.5	1.77	1.18	1.00	1.18	0.60
H(7)	2	1.5	1.71	1.14	1.00	1.14	0.58
H(8–12)	10	3.8	7.49	1.97	1.00	1.97	1.00
H(13)	3	2.0	2.73	1.37	1.00	1.37	0.69
H(14)	3	2.0	3.96	1.98	1.00	1.98	1.00
				bpy			
$H_5/H_{5'}$	6	3.0	0.06	0.020	70.00	1.40	0.71
$H_6/H_{6'}$	6	3.0	0.05	0.017	70.00	1.17	0.59

[a] n_H and n_F are the number of protons and fluorines in solution; $n_F = 6$ and $N = n_H + n_F$. I_{raw} is the integrated volume. The concentration correction factor (C_{corr}) is unity for the neat ILs and is defined as the ratio of solute to IL molarities ([IL]/[solute]) for bpy peaks. The concentration correction intensity is $I_{corr} = C_{corr}I_{raw}N/(n_Hn_F)$, and the normalized corrected intensity is $I_{corr,N} = I_{corr}/\max(I_{corr})$.

between the IL anions and cations. By using $\{^1H-^{19}F\}$ HOESY spectra, Lee et al. showed that the cation interactions with the NTf_2^- anions were quite different for cations containing octyl chains relative to homologous cations having isoelectronic ethoxy(ethoxyethyl) chains on the quaternary ammonium or phosphonium cation.[77]

In this study, we observed certain specific interactions between the $Ru^{2+}(bpy)_3$ solute and both the anion and the cation in the HOESY and ROESY spectra, respectively. The interactions observed in the HOESY spectra of our $Ru^{2+}(bpy)_3$–IL solutions lead us to believe that for the case of the solute–solvent interactions in ILs, the distance dependence of the NOE signals tends more toward the shorter than the longer range, in contrast to what is predicted by Gabl et al. for pure ILs.[99,100] In particular, we have observed asymmetry in the interactions between the four unique proton signals from the $Ru^{2+}(bpy)_3$ solute, particularly with the $Pyrr_{10,1}^+/NTf_2^-$ IL. For this case, specific interactions between the IL cation and the $Ru^{2+}(bpy)_3$ solute are observed for two of the four chemically unique bpy ligand protons but not the other two.

We have also performed $\{^1H-^{19}F\}$ HOESY experiments on the four neat ILs, $Pyrr_{4,1}^+/NTf_2^-$, $Pyrr_{10,1}^+/NTf_2^-$, $Im_{4,1}^+/NTf_2^-$, and $Im_{8,1}^+/NTf_2^-$. Though the effects are subtle, because the concentrations of ILs anions and cations are much higher than those for the $Ru^{2+}(bpy)_3$ solute, it is apparent that anion–cation interactions in the neat ILs differ slightly from those in the presence of dilute solutes. Details of the anion–cation interactions from the HOESY spectra of the neat ILs are given in the Supporting Information.

Solute–Anion Interactions: $\{^1H-^{19}F\}$ HOESY Experiments. Heteronuclear NOE intensities for interactions between the ^{19}F nuclei on the NTf_2^- anion with the ^1H nuclei on both the cation and on the $Ru^{2+}(bpy)_3$ solute were measured using the inverse HOESY experiment. The atom numbers from Figure 1 are used to indicate spectral assignments in the HOESY and ROESY spectra of the bpy ligand and the cations. The $\{^1H-^{19}F\}$ HOESY spectra of $Ru^{2+}(bpy)_3$ solutions in each of the four ILs are shown in Figures 2 and 3, with the one-dimensional ^1H spectra plotted above the horizontal axis and the ^{19}F spectra plotted to the left of the 2D contour plots. The individual cross-peak intensities in the $\{^1H-^{19}F\}$ HOESY spectra are a measure of the strength of the interactions between IL anions both with their corresponding cations and with the $Ru^{2+}(bpy)_3$ solutes. The absence of such potential cross-peaks in the HOESY spectra indicates that there are only very weak interactions between the two species.

In Figure 2, the HOESY cross-peaks between the ^{19}F nuclei on the NTf_2^- anion and the protons on the bpy ligand are observed between 7.0 and 8.5 ppm of ^1H chemical shift and represent the intermolecular NOE interactions between the $Ru^{2+}(bpy)_3$ solute and the anion. The stoichiometry of the $Ru^{2+}(bpy)_3$ solute provides for four unique chemical shifts among the 24 protons on the bpy ligand, labeled H_3, H_4, H_5, and H_6. Symmetry between the H_3 and $H_{3'}$, H_4 and $H_{4'}$, H_5 and $H_{5'}$, and H_6 and $H_{6'}$ protons results in identical chemical shifts for each of these pairs. While four singlet peaks are observed in the ^1H spectrum of $Ru^{2+}(bpy)_3$, it is worth noting that the effective spin concentration per peak is 6-fold higher than the solute concentration of 40 mM. The ^{19}F spectrum of the NTf_2^-

dx.doi.org/10.1021/jp509861g | J. Phys. Chem. B XXXX, XXX, XXX–XXX

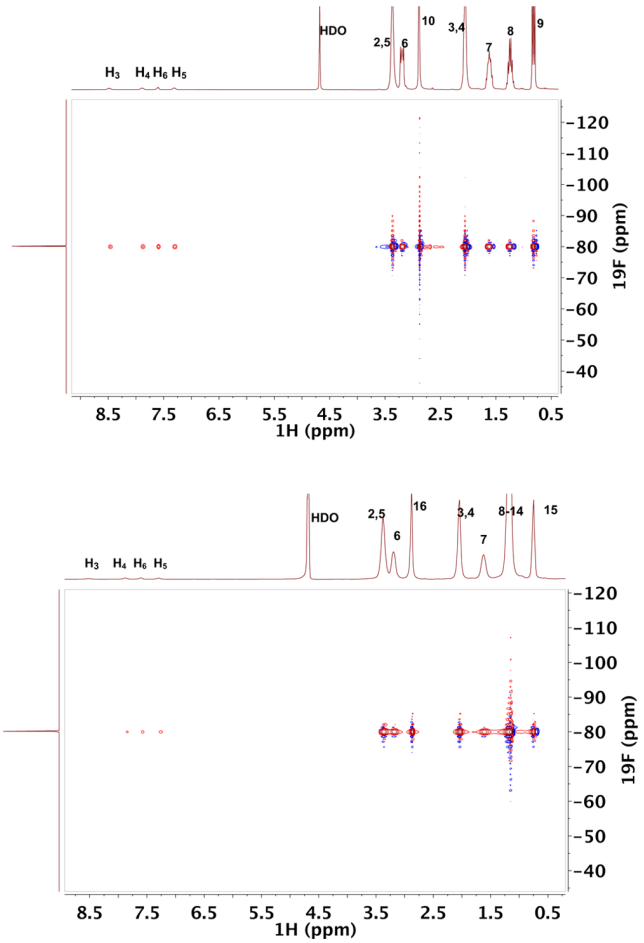

Figure 2. $\{^1H-^{19}F\}$ HOESY spectra of 40 mM $Ru^{2+}(bpy)_3-Cl_2^-$ IL solutions measured at 296 K with 120 ms mixing time. (top) $Pyrr_{4,1}^+/NTf_2^-$ and (bottom) $Pyrr_{10,1}^+/NTf_2^-$. The 1D ^1H and ^{19}F spectra are plotted at the top and left sides of the 2D NOE spectra, respectively.

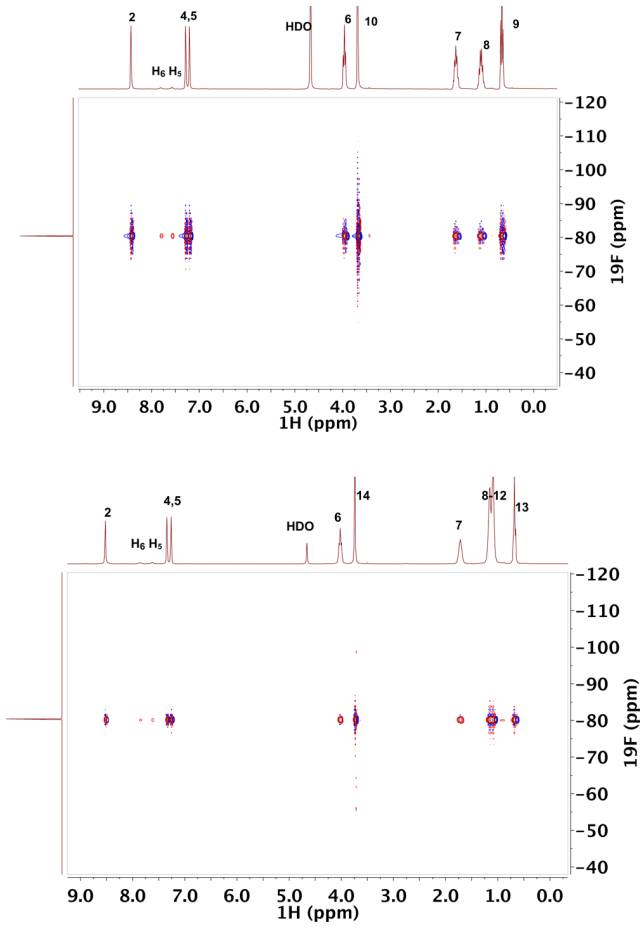

Figure 3. $\{^1H-^{19}F\}$ HOESY spectra of 40 mM $Ru^{2+}(bpy)_3-Cl_2^-$ IL solutions measured at 296 K with 120 ms mixing. (top) $Im_{4,1}^+/NTf_2^-$ and (bottom) $Im_{8,1}^+/NTf_2^-$. The 1D ^1H and ^{19}F spectra are plotted at the top and left sides of the 2D NOE spectra, respectively.

anion presents one singlet peak at −80 ppm chemical shift for the six identical spins. For the pyrrolidinium-cation ILs, the ^1H peaks are observed between 0.7 and 3.5 ppm of chemical shift. Each peak displays strong correlations with the anion ^{19}F peak, so the $\{^1H-^{19}F\}$ HOESY spectra provide a measure of the anion−cation interactions.

The HOESY spectrum in Figure 2 (top) shows that the protons on the bipyridine ligands at H_3, H_4, H_5, and H_6 interact strongly with the ^{19}F nuclei on the NTf_2^- anion for solutions of $Ru^{2+}(bpy)_3$ in $Pyrr_{4,1}^+/NTf_2^-$. This differs from the behavior observed for solutions of $Ru^{2+}(bpy)_3$ in $Pyrr_{10,1}^+/NTf_2^-$. The $^1H-^{19}F$ interactions between $Ru^{2+}(bpy)_3$ in $Pyrr_{10,1}^+/NTf_2^-$ solution are shown in Figure 2 (bottom), where only three of the four bpy protons, H_4, H_5, and H_6, are observed to interact with the NTf_2^- anion.

In Figure 3 (top and bottom), only two of the four bipyridine protons H_5 (7.68 ppm) and H_6 (7.89 ppm) are observed in the HOESY spectra for the two ILs having imidazolium cations, because the chemical shifts for the bpy H_3 and H_4 peaks overlap with those from the imidazolium ring protons.

The corrected integrated and normalized cross-peak volumes for the two solutions with pyrrolidinium-cation ILs are presented in Table 1, and in Table 2 for the imidazolium-cation ILs. These results show that the raw and corrected cross-peak intensities between the bipyridine protons and fluorine nuclei of the NTf_2^- anion, I_{raw} and I_{corr}, display about 3 times more intensity for solutions of $Ru^{2+}(bpy)_3$ in $Pyrr_{4,1}^+/NTf_2^-$ than in $Pyrr_{10,1}^+/NTf_2^-$. Similarly, the bpy solute to anion interactions derived from I_{raw} and I_{corr} in Table 2 are about 3 times stronger for $Ru^{2+}(bpy)_3$ in $Im_{4,1}^+/NTf_2^-$ than in $Im_{8,1}^+/NTf_2^-$ solutions. Thus, the interactions between the NTf_2^- anions and the $Ru^{2+}(bpy)_3$ solutes are significantly decreased when the alkyl chain on the cation is increased from the shorter butyl chain on $Im_{4,1}^+$ or $Pyrr_{4,1}^+$ to the longer octyl chain on $Im_{8,1}^+$ or the decyl chain on $Pyrr_{10,1}^+$. In order to compare spectra for differing numbers of protons among the four ILs, it is important to note that we have chosen to normalize the corrected intensities by the local maximum for each IL, since we do not have the means to calculate a global normalization. A tentative assignment for this effect is that the presence of larger apolar domains for ILs having the longer-chain cations provides an environment in which to solubilize the rather hydrophobic bipyridine ligands of the $Ru^{2+}(bpy)_3$ solute. Recall that the electronic structure of the dicationic solute largely has the positive charge localized near the central Ru^{2+} ion.

The data from the HOESY spectra shown in Figures 2 and 3 are summarized in Tables 1 and 2, respectively. A more pictorial representation of these data is given in Figure 4, where a linear color-intensity scale indicates the strengths of interactions between the anions and both cations and the $Ru^{2+}(bpy)_3$ solutes. Figure 4 makes several points clear. The

dx.doi.org/10.1021/jp509861g | J. Phys. Chem. B XXXX, XXX, XXX−XXX

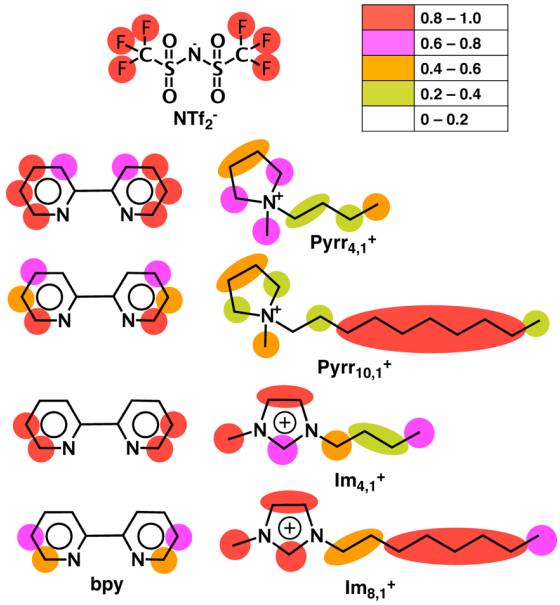

Figure 4. Concentration-corrected, normalized $\{^1H-^{19}F\}$ HOESY spectral intensities $I_{corr,N}$ for 120 ms mixing times, indicating interaction strengths between the NTf_2^- anions and both the IL cations and $Ru^{2+}(bpy)_3$ solutes. Data are from the spectra shown in Figures 2 and 3.

strongest interactions between the fluorine nuclei of the anion with the cation protons are with those protons on the longer decyl tail of $Pyrr_{10,1}^+$ and octyl tail of $Im_{8,1}^+$. The protons on the imidazolium ring and the N-methyl group also interact strongly with the NTf_2^- anion. Overall, the interactions between the bpy ligand with the NTf_2^- anion are stronger for the shorter butyl chain cations than for the two with longer alkyl substituents.

Solute–Cation Interactions: $\{^1H-^1H\}$ ROESY Experiments. The $\{^1H-^1H\}$ ROESY spectra for the solute–IL solutions are shown in Figures 5 and 6 for the pairs of pyrrolidinium-cation and imidazolium-cation ILs, respectively. These spectra indicate strong interactions between IL cations and the bpy protons of $Ru^{2+}(bpy)_3$. The ROESY spectra for these ILs show significant differences between the interactions of the cationic headgroup with another headgroup, and between cationic head and tail groups. Since the NMR signal depends on the solution concentration, solute–cation ROESY cross-peaks are much lower in integrated intensity than cation–cation ROESY cross-peaks, with a lower observed signal-to-noise ratio. The ROESY data show cross-peaks for $\{^1H-^1H\}$ interactions in solution. Because of the richer ^1H spectra of the four cations relative to the single ^{19}F peak for the NTf_2^- anion, the ROESY spectra of the corresponding IL–$Ru^{2+}(bpy)_3$ solutions are significantly more complex than the analogous HOESY spectra. The ROESY spectra of cation–cation interactions for the neat ILs are presented in the Supporting Information. As discussed previously, we observe only intramolecular cation–cation interactions in the ROESY spectra of neat ILs.[77] Thus, we analyze only the integrated intensity of solute–cation cross-peaks. Details of the analysis are given in the Supporting Information.

An overview of the solute–cation interactions for $Ru^{2+}(bpy)_3$ in IL solutions is given in Figure 7. Since there are large variations of integrated ROESY cross-peak intensities between the spectra for the four different IL solutions, we have used a log color scale to represent the ROESY interactions.

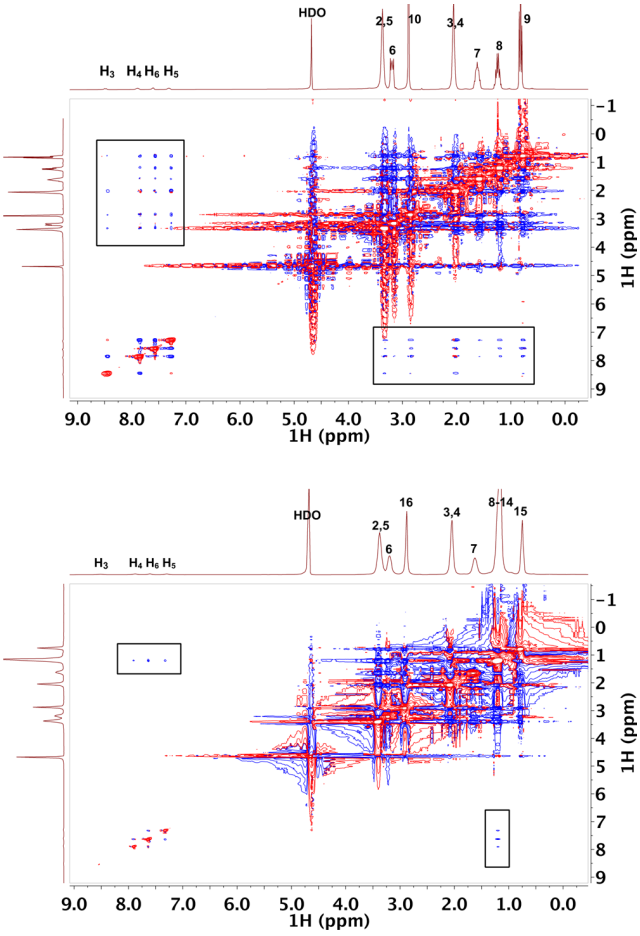

Figure 5. $\{^1H-^1H\}$ homonuclear ROE spectra of 40 mM $Ru^{2+}(bpy)_3-Cl_2^-$ in IL solutions measured at 296 K using a 200 ms mixing time. (top) $Pyrr_{4,1}^+/NTf_2^-$ and (bottom) $Pyrr_{10,1}^+/NTf_2^-$. The 1D ^1H spectra are plotted at the top and left sides of the 2D ROE spectra, respectively.

For the $Ru^{2+}(bpy)_3$ solute in $Pyrr_{4,1}^+/NTf_2^-$ solution, the ROESY spectra indicate that all four bpy protons show strong interactions with both cationic head and tail groups. The H_3 bpy protons interact strongly with $Pyrr_{4,1}^+$ protons at the 3 and 4 positions, while there are comparatively weaker interactions with 2, 5, 9, and 10 protons of $Pyrr_{4,1}^+$ and negligible interactions with protons at the 6, 7, and 8 positions of $Pyrr_{4,1}^+$. The H_4 bpy protons show strong coupling with $Pyrr_{4,1}^+$ protons at the 2, 5, 9, and 10 positions; weak interactions with protons at the 3, 4, 7, and 8 positions; and negligible interactions with the protons at the 6 position. Interactions between the bpy H_5 protons and the $Pyrr_{4,1}^+$ cation are strong for the protons at the cation 3, 4, 8, and 9 positions; weak for the 2, 5, and 7 positions; and negligible for the 6 position. H_6 bpy protons interact strongly with the $Pyrr_{4,1}^+$ protons at the 2–5, 8, 9, and 10 positions and weakly with protons at the 7 position, while negligible interactions are observed for the protons at the 6 position of the cation. We cannot quantitatively compare the intensities between the ROESY and HOESY experiments. However, a qualitative comparison shows that the probabilities of presence about the $Ru^{2+}(bpy)_3$ solute is similar for the NTf_2^- anions and the $Pyrr_{1,4}^+$ cations.

For the solutions of $Ru^{2+}(bpy)_3$ in $Pyrr_{10,1}^+/NTf_2^-$, the ROESY spectra show that protons on the bpy ligands are in

dx.doi.org/10.1021/jp509861g | J. Phys. Chem. B XXXX, XXX, XXX–XXX

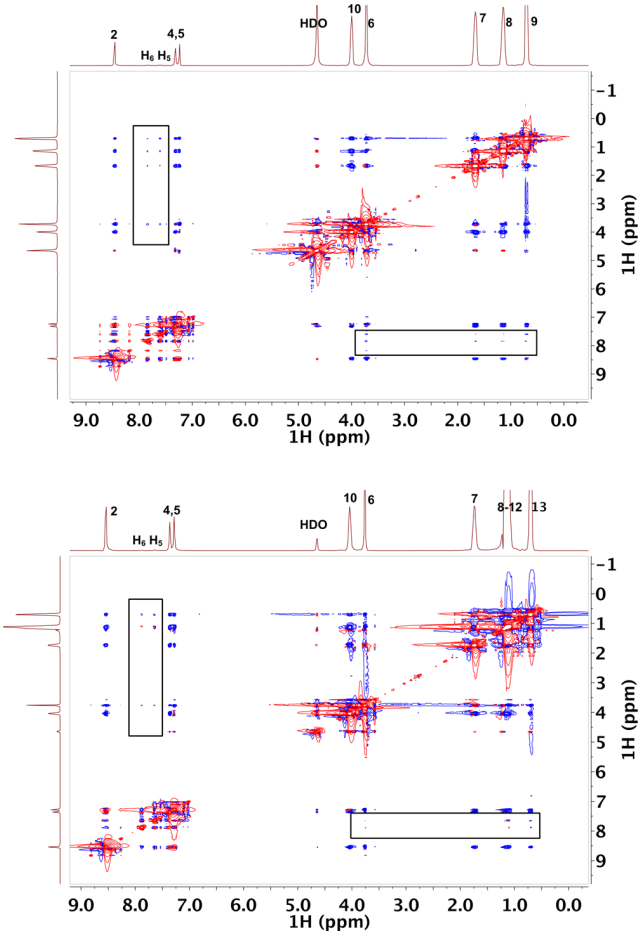

Figure 6. $\{^1H-^1H\}$ ROESY spectra for 40 mM $Ru^{2+}(bpy)_3-Cl_2^-$ solutions in ILs, measured at 296 K with 200 ms mixing times. (top) $Im_{4,1}^+/NTf_2^-$ and (bottom) $Im_{8,1}^+/NTf_2^-$. The 1D ^1H spectra are plotted at the top and left sides of the 2D ROE spectra, respectively.

proximity to the cationic alkyl tail but have negligible interactions with the polar headgroup of the cation. Both the H_5 and H_6 bpy protons show strong interactions with the $Pyrr_{10,1}^+$ cation, specifically with the protons on the methylene groups at positions 8−14. However, no detectable signals above the noise baseline were observed for interactions with these H_5 and H_6 bpy protons and any of the other protons on the $Pyrr_{10,1}^+$ cation. The bpy H_4 protons present weak interactions with these same cationic protons at the 8−14 positions, while no interactions are observed between H_4 and any of the other $Pyrr_{10,1}^+$ protons. No interactions were detected between the bpy H_3 protons and any cationic protons on $Pyrr_{10,1}^+$ in this ROESY spectrum.

Figures 5 and 6 illustrate how the solute−cation interactions are different for the pyrrolidinium-cation IL solutions than for the imidazolium-cation IL solutions. For the imidazolium cations, significant solute−cation interactions are observed between the bpy solute protons with both the polar aromatic ring as well as the nonpolar alkyl substituents. The solute−cation interactions in solution with pyrrolidinium-cation ILs are comparatively stronger than the corresponding interactions in solutions of imidazolium-cation ILs. The relative raw, normalized and corrected intensities are tabulated in the Supporting Information. Solute−cation interactions for the imidazolium-cation ILs are only observed for the H_5 and H_6 bpy protons, which were the same protons observed to interact strongly with the NTf_2^- anion.

For $Ru^{2+}(bpy)_3$ in $Im_{4,1}^+/NTf_2^-$ solution, the bpy H_5 protons interact strongly with the $Im_{4,1}^+$ protons at the imidazolium ring 4 and 5 positions and weakly with protons at the imidazolium ring 2 position, while negligible interactions between bpy and the $Im_{4,1}^+$ cation are observed for protons at the $Im_{4,1}^+$ 7−10 positions. The bpy protons at the H_6 position show weak interactions with the $Im_{4,1}^+$ protons at the 2, 4, and 5 positions and negligible interactions with protons at the $Im_{4,1}^+$ 7−10 positions. No interactions between the bpy and the $Im_{4,1}^+$ protons at the 6 position are observed in these ROESY spectra.

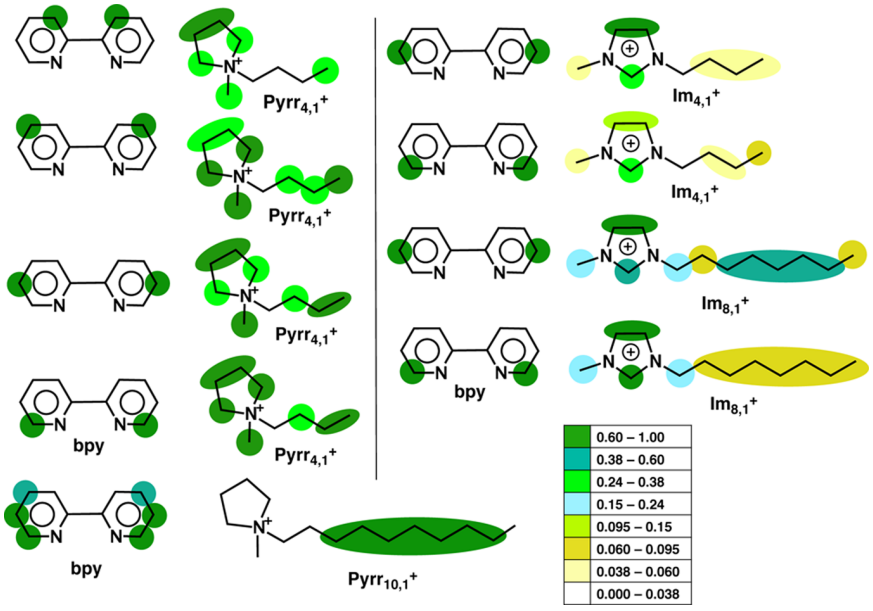

Figure 7. Concentration-corrected, normalized $\{^1H-^1H\}$ ROESY spectral intensities $I_{corr,N}$ for 200 ms mixing times indicating interaction strengths between IL cations and the $Ru^{2+}(bpy)_3$ solute. Data from the spectra shown in Figures 5 and 6.

dx.doi.org/10.1021/jp509861g | J. Phys. Chem. B XXXX, XXX, XXX−XXX

For $Ru^{2+}(bpy)_3$ solutions in $Im_{8,1}^+/NTf_2^-$, the bpy protons at the H_5 position show stronger interactions with the $Im_{8,1}^+$ protons at the 4 and 5 positions on the imidazolium ring relative to the other protons on the $Im_{8,1}^+$ cation. The bpy protons at the H_6 position interact strongly with $Im_{8,1}^+$ protons at the 2, 4, and 5 positions. The relative strength of these interactions is shown in Figure 7. It is intriguing to consider the fact that the signal strengths for the interactions between the cationic methlyene protons labeled "6", located at the junction between the ring nitrogen and the butyl, octyl, or decyl chain, all show no ROESY signal intensities with any of the protons on the bpy ligand of the $Ru^{2+}(bpy)_3$ solute. This could be evidence for some longer-range distance dependence of NOE signals in IL solutions, as has been indicated may be possible in the work of Gabl et al.[99,100] Another possibility is that these cationic methylene protons are typically sterically screened from interactions with the bpy protons on the solute. One reason to give this latter possibility serious consideration is the fact that the HOESY spectra for these ILs show negligible interactions between these same cationic protons and the fluorine nuclei of the NTf_2^- anions.[71,72,78]

The ROESY spectra of the solutions with pyrrolidinium-cation ILs suggest that the alkyl tail of $Pyrr_{10,1}^+$ interacts strongly with the bpy ligands on the $Ru^{2+}(bpy)_3$ solute. In contrast, all of the protons on the $Pyrr_{4,1}^+$ cation show signficant interactions with all four of the bpy protons of $Ru^{2+}(bpy)_3$. For the imidazolium-cation ILs, less information is available because of the spectral overlap between imidazolium ring protons and two of the four bpy protons. While the H_5 and H_6 protons of the bpy ligands do show interactions with the $Im_{8,1}^+$ octyl tail, these interactions are not as strong as those with the imidazolium protons at the 2, 4, and 5 ring positions. This indicates the possibility of aromatic $\pi-\pi$ interactions between the bpy ligands of the solute and the imidazolium ring. This type of interaction has also been suggested by the molecular dynamics results from Terranova and Corcelli, where they saw an enhancement in the radial distribution function for $Im_{2,1}^+$ cations surrounding an aromatic coumarin 153 solute relative to the BF_4^- anions.[64]

CONCLUSIONS

Tantalizing insights into the specific solute−solvent interactions are obtained from analysis of the 2D NOE NMR spectra of solutions of the prototypical photosensitizer, $Ru^{2+}(bpy)_3$, and the anions and cations of the ionic liquid solvents. Diffraction methods and molecular simulations have provided detailed insights into the local structure of bulk ionic liquids. However, both the present experimental results and results from molecular dynamics simulations make clear that the liquid structure immediately surrounding the solute is significantly different from the bulk, especially for ILs having longer cationic alkyl chains.

Several specific insights have been revealed by the 2D NMR spectra. Interactions between the ionic liquid anions with both the $Ru^{2+}(bpy)_3$ solute and the IL cations are probed using the heteronuclear $\{^1H-^{19}F\}$ HOESY method. The HOESY spectra reveal that the interactions between the NTf_2^- anions and the $Ru^{2+}(bpy)_3$ solute are approximately 3 times stronger for the cations with shorter butyl substituents, $Pyrr_{4,1}^+$ and $Im_{4,1}^+$, relative to the cations with longer alkyl chains, $Im_{8,1}^+$ and $Pyrr_{10,1}^+$. Anion−solute interactions have significant intensity for all of the protons on the solute bpy ligands in $Pyrr_{4,1}^+/NTf_2^-$ and for all but the H_3 bpy protons for $Pyrr_{10,1}^+/NTf_2^-$. However, in both the $Im_{4,1}^+/NTf_2^-$ and $Im_{8,1}^+/NTf_2^-$ ILs, solute−anion interactions can only be observed for the H_5 and H_6 bpy protons because of the spectral overlap between the H_3 and H_4 bpy protons with the imidazolium ring protons at the 4 and 5 positions. Anion−cation interactions are observed for all of the cation protons in each of the four ILs. However, the most intense anion−cation interactions are observed between the ^{19}F nuclei of the NTf_2^- anion and the methylene groups on the longer alkyl tails of the $Im_{8,1}^+$ and $Pyrr_{10,1}^+$ cations.

Homonuclear ^1H ROESY spectra provide a means for investigating the interactions between the IL cations and the $Ru^{2+}(bpy)_3$ solutes. Because of the difficulty in separating intra- vs intermolecular signals in ROESY spectra, it is not possible to investigate the cation−cation interactions directly. The fact that the six fluorine atoms on the NTf_2^- anion appear as one singlet peak in the ^{19}F spectrum means that there are no cross-peaks to be observed in the $\{^{19}F-^{19}F\}$ ROESY spectrum. However, the $\{^1H-^1H\}$ ROESY spectra provide significant insights. We have observed that each of the protons on the $Pyrr_{4,1}^+$ cation shows strong interactions with each of the four proton peaks on the bpy ligand. In contrast, the $Pyrr_{10,1}^+$ cation shows interactions with all but the H_3 bpy protons, but only interactions between the methylene groups on the cationic decyl tail are observed. For the two aromatic imidazolium cations $Im_{4,1}^+$ and $Im_{8,1}^+$, interactions can only be observed between the IL cations and the H_5 and H_6 bpy protons. Cation−solute interactions for the imidazoliums with the bpy protons are strongest for the ring protons at the 2, 4, and 5 positions of the imidazolium rings.

While the interactions probed in the 2D NMR experiments are highly averaged, the fact that strong specific interactions are observed between the 40 mM concentration solutes and both the IL anions and cations indicates that these NOE methods do provide specific insights into the unique nature of the solute−ion interactions in IL solutions. More significantly, the interactions observed are rather different than would be expected on the basis of our understanding of bulk ionic liquid structures. The experimental time scales for the NMR experiments extend to seconds, so that direct molecular simulations of the NOE observable are not feasible. Additional experimental insights into specific solute−anion and solute−cation interactions can be studied using molecular simulations, as well as carefully designed resonant X-ray and neutron diffraction experiments. Given that the solute−IL interactions observed to date have all been significantly different than would be projected from bulk IL structures, it seems increasingly important to continue to develop further experimental and theoretical methods for probing specific solvation effects in ionic liquids.

ASSOCIATED CONTENT

Supporting Information

The graph of the heteronuclear NOE intensity as a function of mixing time, as well as the full analysis of the 2D HOESY spectra for a 40 ms mixing time, together with complete tables of all HOESY and ROESY intensities. This material is available free of charge via the Internet at http://pubs.acs.org.

AUTHOR INFORMATION

Corresponding Author

*E-mail: ed.castner@rutgers.edu.

Notes

The authors declare no competing financial interest.

■ ACKNOWLEDGMENTS

We gratefully acknowledge support for this work from the U.S. Department of Energy, Office of Basic Energy Sciences, Division of Chemical Sciences, Geosciences, and Biosciences under contract DE-SC0001780 at Rutgers. We thank Dr. Nagarajan Murali for help in the initial setup of the 2D NMR experiments with the fast autoswitching probe.

■ REFERENCES

(1) Wasserscheid, P.; Keim, W. Ionic Liquids - New "Solutions" for Transition Metal Catalysis. *Angew. Chem., Int. Ed.* **2000**, *39*, 3772−3789.

(2) Riisager, A.; Fehrmann, R.; Haumann, M.; Wasserscheid, P. Supported Ionic Liquid Phase (SILP) Catalysis: An Innovative Concept for Homogeneous Catalysis in Continuous Fixed-Bed Reactors. *Eur. J. Inorg. Chem.* **2006**, 695−706.

(3) Dupont, J. From Molten Salts to Ionic Liquids: A "Nano" Journey. *Acc. Chem. Res.* **2011**, *44*, 1223−1231.

(4) Macfarlane, D. R.; Forsyth, M.; Howlett, P. C.; Pringle, J. M.; Sun, J.; Annat, G.; Neil, W.; Izgorodina, E. I. Ionic Liquids in Electrochemical Devices and Processes: Managing Interfacial Electrochemistry. *Acc. Chem. Res.* **2007**, *40*, 1165−1173.

(5) Armand, M.; Endres, F.; MacFarlane, D. R.; Ohno, H.; Scrosati, B. Ionic-Liquid Materials for the Electrochemical Challenges of the Future. *Nat. Mater.* **2009**, *8*, 621−629.

(6) Swatloski, R.; Spear, S.; Holbrey, J.; Rogers, R. Dissolution of Cellose with Ionic Liquids. *J. Am. Chem. Soc.* **2002**, *124*, 4974−4975.

(7) Tan, S. S. Y.; MacFarlane, D. R.; Upfal, J.; Edye, L. A.; Doherty, W. O. S.; Patti, A. F.; Pringle, J. M.; Scott, J. L. Extraction of Lignin from Lignocellulose at Atmospheric Pressure Using Alkylbenzenesulfonate Ionic Liquids. *Green Chem.* **2009**, *11*, 339−345.

(8) Li, C.; Knierim, B.; Manisseri, C.; Arora, R.; Scheller, H. V.; Auer, M.; Vogel, K. P.; Simmons, B. A.; Singh, S. Comparison of Dilute Acid and Ionic Liquid Pretreatment of Switchgrass: Biomass Recalcitrance, Delignification and Enzymatic Saccharification. *Bioresour. Technol.* **2010**, *101*, 4900−4906.

(9) Anderson, J. L.; Dixon, J. K.; Brennecke, J. F. Solubility of CO2, CH4, C2H6, C2H4, O2, and N2 in 1-Hexyl-3-methylpyridinium Bis(trifluoromethylsulfonyl)imide: Comparison to Other Ionic Liquids. *Acc. Chem. Res.* **2007**, *40*, 1208−1216.

(10) Han, X.; Armstrong, D. W. Ionic Liquids in Separations. *Acc. Chem. Res.* **2007**, *40*, 1079−1086.

(11) Gurkan, B.; Goodrich, B. F.; Mindrup, E. M.; Ficke, L. E.; Massel, M.; Seo, S.; Senftle, T. P.; Wu, H.; Glaser, M. F.; Shah, J. K.; Maginn, E. J.; Brennecke, J. F.; Schneider, W. F. Molecular Design of High Capacity, Low Viscosity, Chemically Tunable Ionic Liquids for CO2 Capture. *J. Phys. Chem. Lett.* **2010**, *1*, 3494−3499.

(12) Plechkova, N. V.; Seddon, K. R. Applications of Ionic Liquids in the Chemical Industry. *Chem. Soc. Rev.* **2008**, *37*, 123−150.

(13) Hallett, J. P.; Welton, T. Room-Temperature Ionic Liquids: Solvents for Synthesis and Catalysis. 2. *Chem. Rev.* **2011**, *111*, 3508−3576.

(14) Smiglak, M.; Pringle, J. M.; Lu, X.; Han, L.; Zhang, S.; Gao, H.; MacFarlane, D. R.; Rogers, R. D. Ionic Liquids for Energy, Materials, and Medicine. *Chem. Commun.* **2014**, *50*, 9228−9250.

(15) Wishart, J. F. Energy Applications of Ionic Liquids. *Energy Environ. Sci.* **2009**, *2*, 956−961.

(16) Bowron, D. T.; Hardacre, C.; Holbrey, J. D.; McMath, S. E. J.; Nieuwenhuyzen, M.; Soper, A. K. Ionic Liquids as Green Solvents: Progress and Prospects. *ACS Symp. Ser.* **2003**, *856*, 151−161.

(17) Triolo, A.; Russina, O.; Bleif, H.-J.; Di Cola, E. Nanoscale Segregation in Room Temperature Ionic Liquids. *J. Phys. Chem. B* **2007**, *111*, 4641−4644.

(18) Russina, O.; Triolo, A.; Gontrani, L.; Caminiti, R.; Xiao, D.; Hines, L. G., Jr.; Bartsch, R. A.; Quitevis, E. L.; Pleckhova, N.; Seddon, K. R. Morphology and Intermolecular Dynamics of 1-Alkyl-3-Methylimidazolium Bis(trifluoromethane)sulfonylamide Ionic Liquids: Structural and Dynamic Evidence of Nanoscale Segregation. *J. Phys.: Condens. Matter* **2009**, *21*, 424121.

(19) Fujii, K.; Kanzaki, R.; Takamuku, T.; Kameda, Y.; Kohara, S.; Kanakubo, M.; Shibayama, M.; Ishiguro, S.-i.; Umebayashi, Y. Experimental Evidences for Molecular Origin of Low-Q Peak in Neutron/X-ray Scattering of 1-Alkyl-3-Methylimidazolium Bis-(trifluoromethanesulfonyl)amide Ionic Liquids. *J. Chem. Phys.* **2011**, *135*, 244502.

(20) Santos, C. S.; Murthy, N. S.; Baker, G. A.; Castner, E. W., Jr. X-ray Scattering from Ionic Liquids with Pyrrollidinium Cations. *J. Chem. Phys.* **2011**, *134*, 121101.

(21) Santos, C. S.; Murthy, N. S.; Baker, G. A.; C, E. W., Jr. Communication: X-ray Scattering from Ionic Liquids with Pyrrolidinium Cations. *J. Chem. Phys.* **2011**, *134*, 121101.

(22) Urahata, S. M.; Ribeiro, M. C. C. Structure of Ionic Liquids Of 1-Alkyl-3-Methylimidazolium Cations: A Systematic Computer Simulation Study. *J. Chem. Phys.* **2004**, *120*, 1855−1863.

(23) Del Popolo, M. G.; Voth, G. A. On the Structure and Dynamics of Ionic Liquids. *J. Phys. Chem. B* **2004**, *108*, 1744−1752.

(24) Canongia Lopes, J. N.; Padua, A. A. H. Nanostructural Organization in Ionic Liquids. *J. Phys. Chem. B* **2006**, *110*, 3330−3335.

(25) Triolo, A.; Russina, O.; Fazio, B.; Triolo, R.; Cola, E. D. Morphology of 1-Alkyl-3-Methylimidazolium Hexafluorophosphate Room Temperature Ionic Liquids. *Chem. Phys. Lett.* **2008**, *457*, 362−365.

(26) Canongia Lopes, J. N.; Shimizu, K.; Padua, A. A. H.; Umebayashi, Y.; Fukuda, S.; Fujii, K.; Ishiguro, S.-i. A Tale of Two Ions:? The Conformational Landscapes of Bis-(trifluoromethanesulfonyl)amide and N,N-Dialkylpyrrolidinium. *J. Phys. Chem. B* **2008**, *112*, 1465−1472.

(27) Fujii, K.; Soejima, Y.; Kyoshoin, Y.; Fukuda, S.; Kanzaki, R.; Umebayashi, Y.; Yamaguchi, T.; Ishiguro, S.-i.; Takamuku, T. Liquid Structure of Room-Temperature Ionic Liquid, 1-ethyl-3-methylimidazolium Bis(trifluoromethanesulfonyl)imides. *J. Phys. Chem. B* **2008**, *112*, 4329−4336.

(28) Fujii, K.; Seki, S.; Fukuda, S.; Takamuku, T.; Kohara, S.; Kameda, Y.; Umebayashi, Y.; i. Ishiguro, S. Liquid Structure and Conformation of a Low-viscosity Ionic Liquid, N-methyl-N-propylpyrrolidinium Bis(trifluorosulfonyl) Imide Studies by High-energy X-ray Scattering. *J. Mol. Liq.* **2008**, *143*, 64−69.

(29) Fukuda, S.; Takeuchi, M.; Fujii, K.; Kanzaki, R.; Takamuku, T.; Chiba, K.; Yamamoto, H.; Umebayashi, Y.; Ishiguro, S.-i. Liquid Structure of N-butyl-N-methylpyrrolidinium Bis-(trifluoromethanesulfonyl) amide Ionic Liquid Studied by Large Angle X-ray Scattering and Molecular Dynamics Simulations. *J. Mol. Liq.* **2008**, *143*, 2−7.

(30) Triolo, A.; Russina, O.; Caminiti, R.; Shirota, H.; Lee, H. Y.; Santos, C. S.; Murthy, N. S.; Castner, E. W., Jr. Comparing Intermediate Range Order for Alkyl- vs. Ether-Substituted Cations in Ionic Liquids. *Chem. Commun.* **2012**, *48*, 4959−4961.

(31) Kashyap, H. K.; Santos, C. S.; Annapureddy, H. V. R.; Murthy, N. S.; Margulis, C. J.; Castner, E. W., Jr. Temperature-Dependent Structure of Ionic Liquids: X-ray Scattering and Simulations. *Faraday Discuss.* **2012**, *154*, 133−143.

(32) Kashyap, H. K.; Hettige, J.; Jeevapani; Anapurredy, H. V.; Margulis, C. J. SAXS Anti-peaks Reveal the Length-scales of Dual Positive−negative and Polar−apolar Ordering in Room-temperature Ionic Liquids. *Chem. Commun.* **2012**, *48*, 5103−5105.

(33) Kashyap, H. K.; Santos, C. S.; Daly, R. P.; Hettige, J.; Murthy, N. S.; Shirota, H.; Castner, E. W., Jr.; Margulis, C. J. How Does the Ionic Liquid Organizational Landscape Change when Nonpolar Cationic Alkyl Groups Are Replaced by Polar Isoelectronic Diethers? *J. Phys. Chem. B* **2013**, *117*, 1130−1135.

(34) Kashyap, H. K.; Santos, C. S.; Murthy, N. S.; et al. Structure of 1-Alkyl-1-methylpyrrolidinium Bis(trifluoromethylsulfonyl)amide Ionic Liquids with Linear, Branched, and Cyclic Alkyl Groups. *J. Phys. Chem. B* **2013**, *117*, 15328−15337.

(35) Antony, J. H.; Mertens, D.; Dolle, A.; Wasserscheid, P.; Carper, W. R. Molecular Reorientational Dynamics of the Neat Ionic Liquid 1-

butyl-3-methylimidazolium Hexafluorophosphate by Measurement of C-13 Nuclear Magnetic Relaxation Data. *ChemPhysChem* **2003**, *4*, 588−594.
(36) Bitrian, V.; Trullas, J.; Silbert, M.; Enosaki, T.; Kawakita, Y.; Takeda, S. Neutron Diffraction Data And Molecular Dynamics Simulations Of The Molten Mixture $Ag(Br_{0.7}I_{0.3})$. *J. Chem. Phys.* **2006**, *125*, 184510.
(37) Dommert, F.; Schmidt, J.; Qiao, B.; Zhao, Y.; Krekeler, C.; Delle Site, L.; Berger, R.; Holm, C. A Comparative Study Of Two Classical Force Fields On Statics And Dynamics Of [Emim][BF4] Investigated Via Molecular Dynamics Simulations. *J. Chem. Phys.* **2008**, *129*, 224501.
(38) Chung, S. H.; Lopato, R.; Greenbaum, S. G.; Shirota, H.; Castner, E. W., Jr.; Wishart, J. F. Nuclear Magnetic Resonance Study of the Dynamics of Imidazolium Ionic Liquids with $CH_2Si(CH_3)_3$ vs. $CH_2C(CH_3)_3$ Substituents. *J. Phys. Chem. B* **2007**, *111*, 4885−4893.
(39) Schröder, C.; Wakai, C.; Weingärtner, H.; Steinhauser, O. Collective Rotational Dynamics In Ionic Liquids: A Computational And Experimental Study Of 1-Butyl-3-Methyl-Imidazolium Tetrafluoroborate. *J. Chem. Phys.* **2007**, *126*, 84511.
(40) Sloutskin, E.; Lynden-Bell, R. M.; Balasubramanian, S.; Deutsch, M. The Surface Structure Of Ionic Liquids: Comparing Simulations With X-Ray Measurements. *J. Chem. Phys.* **2006**, *125*, 174715.
(41) Triolo, A.; Russina, O.; Hardacre, C.; Nieuwenhuyzen, M.; Gonzalez, M. A.; Grimm, H. Relaxation Processes in Room Temperature Ionic Liquids: The Case of 1-butyl-3-methylimidazolium Hexafluorophosphate. *J. Phys. Chem. B* **2005**, *109*, 22061−22066.
(42) Hardacre, C.; Holbrey, J. D.; Mullan, C. L.; A, Y. T. G.; Bowron, D. T. Small Angle Neutron Scattering from 1-Alkyl-3-Methylimidazolium Hexafluorophosphate Ionic Liquids ($[C_n mim][PF_6]$, n = 4, 6, and 8). *J. Chem. Phys.* **2010**, *133*, 74510.
(43) Gutel, T.; Santini, C. C.; Padua, A. A. H.; Fenet, B.; Chauvin, Y.; Canongia, L. J. N.; Bayard, F.; Costa, G. M. F.; Pensado, A. S. Interaction between the π-System of Toluene and the Imidazolium Ring of Ionic Liquids: A Combined NMR and Molecular Simulation Study. *J. Phys. Chem. B* **2009**, *113*, 170−177.
(44) Behera, K.; Pandey, M. D.; Porel, M.; Pandey, S. Unique Role Of Hydrophilic Ionic Liquid In Modifying Properties Of Aqueous Triton X-100. *J. Chem. Phys.* **2007**, *127*, 184501.
(45) Domanska, U.; Pobudkowska, A.; Rogalski, M. Surface Tension of Binary Mixtures of Imidazolium and Ammonium Based Ionic Liquids with Alcohols, or Water: Cation, Anion Effect. *J. Colloid Interface Sci.* **2008**, *322*, 342−350.
(46) Holbrey, J. D.; Reichert, W. M.; Nieuwenhuyzen, M.; Sheppard, O.; Hardacre, C.; Rogers, R. D. Liquid Clathrate Formation in Ionic Liquid-aromatic Mixtures. *Chem. Commun.* **2003**, 476−477.
(47) Huddleston, J. G.; Willauer, H. D.; Swatloski, R. P.; Visser, A. E.; Rogers, R. D. Room Temperature Ionic Liquids as Novel Media for 'Clean' Liquid-liquid Extraction. *Chem. Commun.* **1998**, 1765−1766.
(48) Kossmann, S.; Thar, J.; Kirchner, B.; Hunt, P.; Welton, T. Cooperativity In Ionic Liquids. *J. Chem. Phys.* **2006**, *124*, 174506.
(49) Umebayashi, Y.; Jiang, J.-C.; Shan, Y.-L.; Lin, K.-H.; Fujii, K.; Seki, S.; Ishiguro, S.-I.; Lin, S. H.; Chang, H.-C. Structural Change Of Ionic Association In Ionic Liquid/Water Mixtures: A High-Pressure Infrared Spectroscopic Study. *J. Chem. Phys.* **2009**, *130*, 124503.
(50) Castriota, M.; Caruso, T.; Agostino, R. G.; Cazzanelli, E.; Henderson, W. A.; Passerini, S. Raman Investigation of the Ionic Liquid N-methyl-N-propylpyrrolidinium Bis-(trifluoromethanesulfonyl)imide and its Mixture with $LiN(SO_2CF_3)_2$. *J. Phys. Chem. A* **2005**, *109*, 92−96.
(51) Castner, E. W., Jr.; Margulis, C. J.; Maroncelli, M.; Wishart, J. F. Ionic Liquids: Structure and Photochemical Reactions. *Annu. Rev. Phys. Chem.* **2011**, *62*, 85−105.
(52) Castner, E. W., Jr.; Wishart, J. F.; Shirota, H. Intermolecular Dynamics, Interactions, and Solvation in Ionic Liquids. *Acc. Chem. Res.* **2007**, *40*, 1217−1227.
(53) Holbrey, J. D.; Seddon, K. R. The Phase Behaviour of 1-alkyl-3-methylimidazolium Tetrafluoroborates; Ionic Liquids and Ionic Liquid Crystals. *J. Chem. Soc., Dalton Trans.* **1999**, 2133−2139.
(54) Mali, K.; Dutt, G.; Mukherjee, T. Do Organic Solutes Experience Specific Interactions With Ionic Liquids? *J. Chem. Phys.* **2005**, *123*, 174504.
(55) Mali, K. S.; Dutt, G. B.; Mukherjee, T. Rotational Diffusion Of A Nonpolar And A Dipolar Solute In 1-Butyl-3-Methylimidazolium Hexafluorophosphate And Glycerol: Interplay Of Size Effects And Specific Interactions. *J. Chem. Phys.* **2008**, *128*, 054504.
(56) MacFarlane, D. R.; Forsyth, S. A. *Ionic Liquids as Green Solvents: Progress and Prospects*; ACS Symposium Series; American Chemical Society: Washington, DC, **2003**; Vol. *856*, pp 264−276.
(57) Fort, D. A.; Swatloski, R. P.; Moyna, P.; Rogers, R. D.; Moyna, G. Use of Ionic Liquids in the Study of Fruit Ripening by High-resolution ^{13}C NMR Spectroscopy: 'Green' Solvents Meet Green Bananas. *Chem. Commun.* **2006**, 714−716.
(58) Wishart, J. F. In *Ionic Liquids as Green Solvents: Progress and Prospects*; Rodgers, R. D., Seddon, K. R., Eds.; ACS Symposium Series; American Chemical Society: Washington, DC, **2003**; Vol. *856*, pp 381−396.
(59) Crowhurst, L.; Mawdsley, P. R.; Perez-Arlandis, J. M.; Salter, P. A.; Welton, T. Solvent-solute Interactions in Ionic Liquids. *Phys. Chem. Chem. Phys.* **2003**, *5*, 2790−2794.
(60) Pádua, A. A. H.; Costa Gomes, M. F.; Canongia Lopes, J. N. A. Molecular Solutes in Ionic Liquids: A Structural Perspective. *Acc. Chem. Res.* **2007**, *40*, 1087−1096.
(61) Crowhurst, L.; Lancaster, N. L.; Perez-Arlandis, J. M.; Welton, T. *Ionic Liquids IIIB: Fundamentals, Progress, Challenges and Opportunities: Transformations and Processes*; ACS Symposium Series; American Chemical Society: Washington, DC, 2005; Vol. *902*, pp 218−232.
(62) Welton, T. Room-temperature Ionic Liquids. Solvents for Synthesis and Catalysis. *Chem. Rev.* **1999**, *99*, 2071−2083.
(63) Hardacre, C.; Holbrey, J. D.; Nieuwenhuyzen, M.; Youngs, T. G. A. Structure and Solvation in Ionic Liquids. *Acc. Chem. Res.* **2007**, *40*, 1146−1155.
(64) Terranova, Z. L.; Corcelli, S. A. On the Mechanism of Solvation Dynamics in Imidazolium-Based Ionic Liquids. *J. Phys. Chem. B* **2013**, *117* (49), 15659−15666.
(65) Znamenskiy, V.; Kobrak, M. N. Molecular Dynamics Study of Polarity in Room-temperature Ionic Liquids. *J. Phys. Chem. B* **2004**, *108*, 1072−1079.
(66) Bauer, W. Pulse Field Gradient 'Inverse' HOESY Applied to the Isotope Pairs H-1, P-31 and H-1, Li-7. *Magn. Reson. Chem.* **1996**, *34*, 532.
(67) Ghys, L.; Biesemans, M.; Gielen, M.; Garoufis, A.; Hadjiliadis, N.; Willem, R.; Martins, J. C. Multinuclear 1D and 2D NMR Investigations on the Interaction between the Pyrimidic Nucleotides 5′-CMP, 5′-dCMP, and 5′-UMP and Diethyltin Dichloride in Aqueous Medium. *Eur. J. Inorg. Chem.* **2000**, 513−522.
(68) Alam, T. M.; Pedrotty, D. M.; Boyle, T. Modified, Pulse Field Gradient-Enhanced Inverse-Detected HOESY Pulse Sequence for Reduction of T1 Spectral Artifacts. *Magn. Reson. Chem.* **2002**, *40*, 361−365.
(69) Macchioni, A. Elucidation of the Solution Structures of Transition Metal Complex Ion Pairs by NOE NMR Experiments. *Eur. J. Inorg. Chem.* **2003**, 195−205.
(70) Nama, D.; Kumar, P. G. A.; Pregosin, P. S.; Geldbach, T. J.; Dyson, P. J. H-1, F-19-HOESY and PGSE Diffusion Studies on Ionic Liquids: The Effect of Co-Solvent on Structures. *Inorg. Chem. Acta* **2006**, *359*, 1907−1911.
(71) Castiglione, F.; Moreno, M.; Raos, G.; Famulari, A.; Mele, A.; Appetecchi, G. B.; Passerini, S. Structural Organization and Transport Properties of Novel Pyrrolidinium-Based Ionic Liquids with Perfluoroalkyl Sulfonylimide Anions. *J. Phys. Chem. B* **2009**, *113*, 10750−10759.
(72) Castiglione, F.; Raos, G.; Appetecchi, G. B.; Montanino, M.; Passerini, S.; Moreno, M.; Famulari, A.; Mele, A. Blending Ionic Liquids: How Physico-chemical Properties Change. *Phys. Chem. Chem. Phys.* **2010**, *12*, 1784−1792.

(73) Hou, S.-S.; Tzeng, J.-K.; Chuang, M.-H. Intermolecular Association and Supramolecular Structures of PNVF-LiPFN and PVP-LiPFN Complexes in the Aqueous Phase. *Soft Matter* **2010**, *6*, 409−415.
(74) Ampt, K. A. M.; Aspers, R. L. E. G.; Jaeger, M.; Geutjes, P. E. T. J.; Honing, M.; Wijmenga, S. S. Application of Fluorine NMR for Structure Identification of Steroids. *Magn. Reson. Chem.* **2011**, *49*, 221−230.
(75) Marincola, F. C.; Piras, C.; Russina, O.; Gontrani, L.; Saba, G.; Lai, A. NMR Investigation of Imidazolium-Based Ionic Liquids and Their Aqueous Mixtures. *ChemPhysChem* **2012**, *13*, 1339−1346.
(76) Lingscheid, Y.; Arenz, S.; Giernoth, R. Heteronuclear NOE Spectroscopy of Ionic Liquids. *ChemPhysChem* **2012**, *13*, 261−266.
(77) Lee, H. Y.; Shirota, H.; Castner, E. W., Jr. Differences in Ion Interactions for Isoelectronic Ionic Liquid Homologs. *J. Phys. Chem. Lett.* **2013**, *4*, 1477−1483.
(78) Chiappe, C.; Sanzone, A.; Mendola, D.; Castiglione, F.; Famulari, A.; Raos, G.; Mele, A. Pyrazolium- versus Imidazolium-Based Ionic Liquids: Structure, Dynamics and Physicochemical Properties. *J. Phys. Chem. B* **2013**, *117*, 668−676.
(79) Lopes, J. N. C.; Gomes, M. F. C.; Padua, A. A. H. Nonpolar, Polar, and Associating Solutes in Ionic Liquids. *J. Phys. Chem. B* **2006**, *110*, 16816−16818.
(80) Pan, Y.; Boyd, L. E.; Kruplak, J. F.; Cleland, W. E. J.; Wilkes, J. S.; Hussey, C. L. J. Physical and Transport Properties of Bis(trifluoromethylsulfonyl)imide-based Room-temperature Ionic Liquids: Application to the Diffusion of Tris(2,2-bipyridyl)ruthenium-(II). *Electrochem. Soc.* **2011**, *158*, F1−F9.
(81) Creutz, C.; Chou, M.; Netzel, T. L.; Okumura, M.; Sutin, N. Lifetimes, Spectra, and Quenching of the Excited-states of Polypyridine Complexes of Iron(II), Ruthenium(II) and Osmium(II). *J. Am. Chem. Soc.* **1980**, *102*, 1309−1319.
(82) Durham, B.; Caspar, J. V.; Nagle, J. K.; Meyer, T. J. Photochemistry of $Ru(bpy)_3^{2+}$. *J. Am. Chem. Soc.* **1982**, *104*, 4803−4810.
(83) Caspar, J. V.; Meyer, T. J. Photochemistry of $Ru(bpy)_3^{2+}$ − Solvent Effects. *J. Am. Chem. Soc.* **1983**, *105*, 5583−5590.
(84) Moon, H. C.; Lodge, T. P.; Frisbie, C. D. Solution-Processable Electrochemiluminescent Ion Gels for Flexible, Low-Voltage, Emissive Displays on Plastic. *J. Am. Chem. Soc.* **2014**, *136*, 3705−3712.
(85) *MestReNova*, Mnova version 8.1.0; Mestrelab Research, S.L.: Feliciano Barrera 9B, Bajo, 15706 Santiago de Compostela, Spain, 2013; http://mestrelab.com/.
(86) Macura, S.; Ernst, R. R. Elucidation of Cross Relaxation in Liquids by Two-dimensional NMR Spectroscopy. *Mol. Phys.* **2002**, *100*, 135−147.
(87) Hardacre, C.; Holbrey, J. D.; McMath, S. E. J.; Bowron, D. T.; Soper, A. K. Structure of Molten 1,3-Dimethylimidazolium Chloride Using Neutron Diffraction. *J. Chem. Phys.* **2003**, *118*, 273−278.
(88) Wang, Y.; Jiang, W.; Yan, T.; Voth, G. A. Understanding Ionic Liquids through Atomistic and Coarse-Grained Molecular Dynamics Simulations. *Acc. Chem. Res.* **2007**, *40*, 1193−1199.
(89) Canongia Lopes, J. N.; Padua, A. A. H.; Shimizu, K. Molecular Force Field for Ionic Liquids IV: Trialkylimidazolium and Alkoxycarbonyl-Imidazolium Cations; Alkylsulfonate and Alkylsulfate Anions. *J. Phys. Chem. B* **2008**, *112*, 5039−5046.
(90) Siqueira, L. J. A.; Ribeiro, M. C. C. Alkoxy Chain Effect on the Viscosity of a Quaternary Ammonium Ionic Liquid: Molecular Dynamics Simulations. *J. Phys. Chem. B* **2009**, *113*, 1074−1079.
(91) Pensado, A. S.; Malfreyt, P.; Padua, A. A. H. Molecular Dynamics Simulations of the Liquid Surface of the Ionic Liquid 1-Hexyl-3-methylimidazolium Bis(trifluoromethanesulfonyl)amide: Structure and Surface Tension. *J. Phys. Chem. B* **2009**, *113*, 14708−14718.
(92) Hyun, B. R.; Dzyuba, S. V.; Bartsch, R. A.; Quitevis, E. L. Intermolecular Dynamics of Room-Temperature Ionic Liquids: Femtosecond Optical Kerr Effect Measurements on 1-alkyl-3-methylimidazolium Bis((trifluoromethyl)sulfonyl)imides. *J. Phys. Chem. A* **2002**, *106*, 7579−7585.
(93) Giraud, G.; Gordon, C.; Dunkin, I.; Wynne, K. The Effects Of Anion And Cation Substitution On The Ultrafast Solvent Dynamics Of Ionic Liquids: A Time-Resolved Optical Kerr-Effect Spectroscopic Study. *J. Chem. Phys.* **2003**, *119*, 464−477.
(94) Ribeiro, M. C. C. Correlation between Quasielastic Raman Scattering and Configurational Entropy in an Ionic Liquid? *J. Phys. Chem. B* **2007**, *111*, 5008−5015.
(95) Xiao, D.; Hines, L. G., Jr.; Li, S.; Bartsch, R. A.; Quitevis, E. L.; Russina, O.; Triolo, A. Effect of Cation Symmetry and Alkyl Chain Length on the Structure and Intermolecular Dynamics of 1,3-Dialkylimidazolium Bis(trifluoromethanesulfonyl)amide Ionic Liquids. *J. Phys. Chem. B* **2009**, *113*, 6426−6433.
(96) Zheng, W.; Mohammend, A.; Hines, L. G., Jr.; Xiao, D.; Martinez, O. J.; Bartsch, R. A.; Simon, S. L.; Russina, O.; Triolo, A.; Quitevis, E. L. Effect of Cation Symmetry on the Morphology and Physicochemical Properties of Imidazolium Ionic Liquids. *J. Phys. Chem. B* **2011**, *115*, 6572−6584.
(97) Shirota, H. Comparison of Low-Frequency Spectra between Aromatic and Nonaromatic Cation Based Ionic Liquids Using Femtosecond Raman-Induced Kerr Effect Spectroscopy. *ChemPhysChem* **2012**, *13*, 1638−1648.
(98) Zuccaccia, C.; Bellachioma, G.; Cardaci, G.; Macchioni, A. Solution Structure Investigation of Ru(II) Complex Ion Pairs: Quantitative NOE Measurements and Determination of Average Interionic Distances. *J. Am. Chem. Soc.* **2001**, *123*, 11020−11028.
(99) Gabl, S.; Steinhauser, O.; Weingartner, H. From Short-range to Long-Range Intermolecular NOEs in Ionic Liquids: Frequency Does Matter. *Angew. Chem.* **2013**, *52*, 1−6.
(100) Gabl, S.; Schrder, C.; Braun, D.; Weingrtner, H.; Steinhauser, O. Pair Dynamics and the Intermolecular Nuclear Overhauser Effect (NOE) in Liquids Analysed by Simulation and Model Theories: Application to an Ionic Liquid. *J. Chem. Phys.* **2014**, *140*, 184503.